

# Optoelectronics for neutron detectors based on superheated emulsions

Andrea Chierici<sup>1,\*</sup>, Francesco d'Errico<sup>1,2</sup>

<sup>1</sup>School of Engineering, University of Pisa, Italy

<sup>2</sup>Italian National Institute of Nuclear Physics, Pisa, Italy

\*andrea.chierici@ing.unipi.it

**Abstract**—This paper presents the design, assembly, and performance investigation of an optoelectronic readout system specifically designed to enhance the real-time readout capabilities of Superheated Drop Detectors (SDDs). SDDs as fast neutron detectors have been widely used in different areas such as homeland security, radiation protection, and personal dosimetry. In homeland security, SDDs showed the potential of detecting prompt fission neutrons from special nuclear materials in radiation portal monitor systems, possibly positioning them as a valuable alternative to He-3 detectors. In radiation protection and personal dosimetry, downsized SDDs may be employed to assess the level of exposure of workers in nuclear energy production facilities or as a tool to perform photoneutron contamination studies of medical and research accelerators. The proposed readout system utilizes light-emitting diodes to illuminate the detectors, while photodiodes are employed to record the integral value of scattered light resulting from bubbles' formation, a consequence of neutron interaction. To validate the behavior of the system, comprehensive field testing was conducted after assembling and integrating it with custom-made 3D printed structures tailored for different SDD geometry, and the reader was utilized to examine the optical and detection characteristics of different SDD compositions under various ionizing radiation conditions. The potential to actively read out SDDs in real-time represents a significant advancement for this radiation detection technology, particularly in fields such as radiation protection and industrial applications, and it provides valuable insights for future enhancements in the field of neutron radiation detection.

**Keywords** —Superheated Drop Detector, Optical Readout, Active Interrogation, Neutron Dosimetry, Homeland Security.

## I. INTRODUCTION

THE increasing need for new neutron detection technologies and their diverse applications have resulted in a growing research effort across several domains, such as homeland security, radiation safety, fusion and fission research, and more [1, 2]. For instance, in the field of national security, neutron detectors can play a critical role in mitigating threats posed by the illicit transport of Special Nuclear Materials (SNM) like <sup>235</sup>U, <sup>237</sup>Np, and <sup>239</sup>Pu [3, 4, 5].

Superheated Droplet Detectors (SDDs) offer several unique advantages compared to other neutron detection technologies, such as size adaptability, passive operation, and gamma-ray insensitivity, making them invaluable in these applications [6, 7, 8]. In active interrogation techniques employed for SNM detection, SDDs' adjustable energy

thresholds and gamma radiation insensitivity enables them to operate as prompt fission neutron detectors without interference from the high energy and flux of the interrogation source.

In the domains of radiation safety and medical contexts, SDDs are interesting tools for personnel dosimetry and photo-neutron contamination studies [9, 10]. The challenge of accurate neutron dose measurement, given the complexities of neutron detection physics and the broad energy range to be covered, is met well by SDDs, whose response curve aligns closely with the International Commission on Radiological Protection (ICRP) equivalent curve across the entire energy range [11]. Indeed, a 1989 research study supported this, demonstrating that the response curve of SDDs followed the ideal ICRP dose equivalent response curve within a minor deviation [12].

Leveraging the inherent property of the superheated liquid in SDDs, neutron spectrometry can also be fine-tuned by controlling the operative thermodynamic parameters of the emulsions, such as temperature and pressure. Additionally, in scenarios involving patient exposure to unwanted neutron doses, SDDs, due to their photon insensitivity, passive operation, tissue-equivalent composition, isotropic response, compact size, and cost-effectiveness, can provide reliable estimations of the spatial and energetic distribution of contamination neutrons.

This paper focuses on the design, realization, testing, and calibration of a fast neutron detection system based on SDDs equipped with dedicated optical readout systems. Different strategies have been pursued for the readout of bubble formation in SDDs, such as acoustic counting or image processing [13, 14]. However, each of these methods comes with its own set of challenges. For instance, acoustic counting, which involves the use of piezoelectric sensors or microphones, is significantly sensitive to environmental noise and vibrations. This can interfere with accurate bubble detection and counting, thus compromising the reliability of the system. On the other hand, image processing, involving the use of digital cameras such as CCD (Charge-Coupled Device) or CMOS (Complementary Metal-Oxide-Semiconductor) sensors, requires a more complex and expensive hardware setup. This complexity not only lies in the level of detection, where high-resolution cameras with precise focus control are required but also extends to the data processing stage. Large volumes of image data need to be processed and analyzed in real-time to detect and count the bubbles accurately, which demands high computational resources.

Considering these challenges, our proposed system offers a promising solution that capitalizes on optical readout systems for SDDs. The wide-ranging applicability of this proposed system spans homeland security, neutron spectrometry, personnel dosimetry, and radiation safety. This underscores its potential as a tool in the detection of prompt fission neutrons in active interrogation techniques, significantly aiding in the prevention of unauthorized SNM transport across national borders.

## II. SUPERHEATED LIQUIDS AND DROPLET DETECTORS

SDDs are engineered utilizing a liquid that exists in a metastable or *superheated* state. Superheating is a process where a liquid remains in a state of unstable equilibrium, not vaporizing even when its temperature exceeds its boiling point but is still below the critical point. This liquid can be dispersed as minuscule droplets embedded within an insoluble host gel matrix or in other words as an *emulsion*, which in turn allows to maintain the liquid's metastable state [7]. These droplets, with diameters varying between 50  $\mu\text{m}$  and 200  $\mu\text{m}$ , can transform into gas bubbles, typically ranging from 1 mm to 2 mm in size (Fig. 1). This vaporization process is caused by the deposition of energy following the interaction of the droplets with charged particles traveling through the emulsion [15, 8].

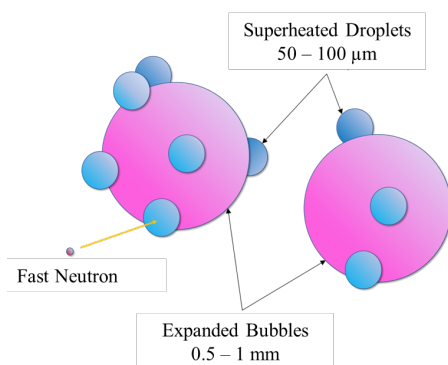


Fig. 1. Superheated Droplet Detectors.

SDDs are predominantly composed of elements such as Hydrogen (H), Carbon (C), Oxygen (O), Fluorine (F), and Chlorine (Cl). The interaction of these elements with neutron scattering leads to the production of energetic recoiled charged particles, which prompts the droplet to vaporize, forming a gas bubble. The unique characteristic of SDDs that renders them insensitive to gamma rays depends on the low linear energy transfer of gamma rays, which prevents them from depositing the requisite energy for vaporization (Fig. 2) [16].

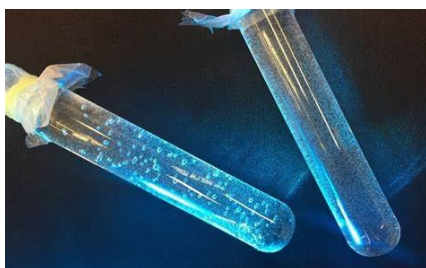


Fig. 2. Superheated Liquid in glass containers in the presence and absence of bubbles following exposure to fast neutrons.

Notably, the threshold energy for SDDs that can be detected can be adjusted not only by modifying the chemical

composition of the detector but also by modifying the operating temperature and pressure of the emulsion. When the temperature rises, both the surface tension and the enthalpy of evaporation decrease, which lowers the minimum energy required for a droplet to vaporize. Similarly, by reducing the operating pressure, the energy necessary for vaporization can be decreased, as reaching the critical radius demands less work under reduced pressure conditions.

## III. OPTICAL READOUT FOR SUPERHEATED EMULSIONS

Our approach leverages an optical readout scattering principle for the detection and quantification of bubbles in neutron detectors. This method involves the use of photodiode arrays and trans-impedance op-amp circuits (Fig. 3) together with LEDs for stimulation.

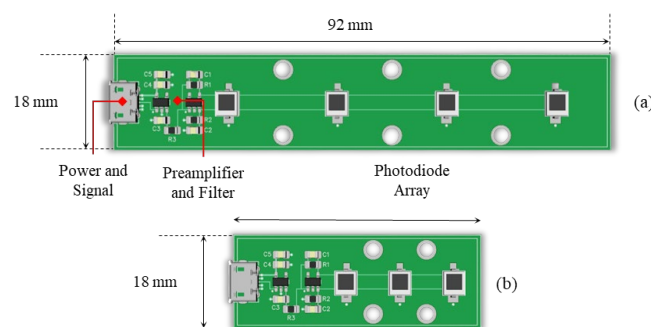


Fig. 3. Transimpedance amplifiers used to read out the lateral optical scattering in large vessels (a) and small vials (b).

TABLE I  
HALOCARBON COMPOSITION AND PROPERTIES

Name	Chemical Formula	Boiling Point (°C)	Critical Temperature (°C)
Octafluorocyclobutane (C318)	C <sub>4</sub> F <sub>8</sub>	-7.0	115.2
Hexafluoropropylene (HFP)	C <sub>3</sub> F <sub>6</sub>	-29.4	85.2
Decafluorobutane (R610)	C <sub>4</sub> F <sub>10</sub>	-1.7	113.3

Due to the large size of the scattering particle, the scattering regime is closely tied to the optical geometry [17]. Although most of the scattering transpires in the forward direction, this light overlaps with transmitted light and does not exhibit a wavelength shift, rendering it impractical for detection purposes. Consequently, we concentrate on the side scattered light, ensuring its proper collimation to exclude the significant, but unwanted, forward component of light. Throughout the project's development, we employed two distinct container geometries: small glass vials of a few milliliters in volume, and larger tempered glass vessels capable of holding several liters, provided by Büchi Labortechnik AG. Given their compact size, the glass vials are ideal for use as personal dosimeters or as distributed detectors in radiation contamination studies. On the other hand, large vessel detectors are constructed from tempered glass that can withstand pressures up to 5 MPa. This strength allows for the adjustment of their operational pressure, enabling selective response to neutrons of various energies and/or resetting the formed bubbles back to a liquid phase. Consequently, as SDDs can be rendered gamma radiation insensitive, they are well-suited as neutron detectors for

active interrogation techniques and neutron spectrometry applications. For this study, halocarbons with a moderate degree of superheat (Table I) were utilized as the superheated liquid, owing to their nucleation exclusively by energetic heavy ions, such as those released by fast neutron interactions [8]. Concerning the optical readout, blue light LEDs (HPWN-MB00, Lumileds Lightning) peaking at 450 nm were chosen because of the superior light output stability versus temperature changes and for the low absorption of blue light in aqueous media [18]. The operation of the LEDs was managed by a self-made Pulse Width Modulation (PWM) driver, which was centered around a TLV431 reference. This reference was arranged to serve as a constant current sink during the high periods of the PWM signal. The nominal current during these "on" phases was adjustable, offering a range between 1.24 mA and 12.4 mA. Furthermore, the PWM frequency could be selected between 2 kHz and 10 kHz. The duty cycle was user-configurable based on the needed average light intensity, offering a selection range from 1% to 10%. These user-configurable parameters, therefore, enabled a vast span of average LED currents, from a minimum of approximately 12.4  $\mu$ A to a maximum of about 1.24 mA, thus ensuring flexibility in adjusting the LED intensity to match the requirements of each experiment.

To convert and amplify the current signals generated from incident light on blue response-enhanced photodiode arrays (BPW34B, Vishay), trans-impedance amplifiers were implemented using TLV341 operational amplifiers (Texas Instruments). The trans-impedance amplifiers consisted of two cascaded operational amplifiers. The first operational amplifier was configured to reject electrostatic coupling by utilizing the Common Mode Rejection Ratio (CMRR) of the op-amp, and it had a gain of 200 kohms to amplify the current signals effectively. The second operational amplifier acted as a buffer for the passive low pass filter set at a cutoff frequency of 15.9 Hz. The output signals from the trans-impedance amplifiers underwent subsequent filtering and digitization. This process was performed by a microcontroller-based data acquisition module. The module provided a resolution of 16 bits and a conversion speed of 1 ksp/s.

The data acquisition module and the controller were directly connected to a personal computer, facilitating control through a dedicated graphical user interface. This enabled convenient interaction and control over the system's functionality.

As discussed, we utilized two different container geometries for the SDDs in this study - glass vials and tempered glass vessel containers. Consequently, we designed and assembled two distinct types of 3D-printed polylactic acid holders to accommodate these different geometries. These holders serve a dual purpose; not only do they provide mechanical support for the optoelectronics printed circuit boards, but they also function as light collimators. To reduce the sensitivity to long-term drifts in the light source and the optical characteristics of the emulsion, a real-time edge detection algorithm was implemented. This was accomplished by processing the detected scattered light signals with a band-pass moving average filter. Each time an uptick in the light signal is registered, the corresponding edge is subsequently reconstituted.

#### A. Readout System for Vial Detectors

In Fig. 4 the design and assembly of the 3D-printed holders used for the glass vial containers are shown. Since vials are relatively small ( $\text{\O}17 \text{ mm} \times 30 \text{ mm}$  active volume), they are well suited to be used both as pocket personal dosimeters and as distributed detectors for radiation contamination studies.

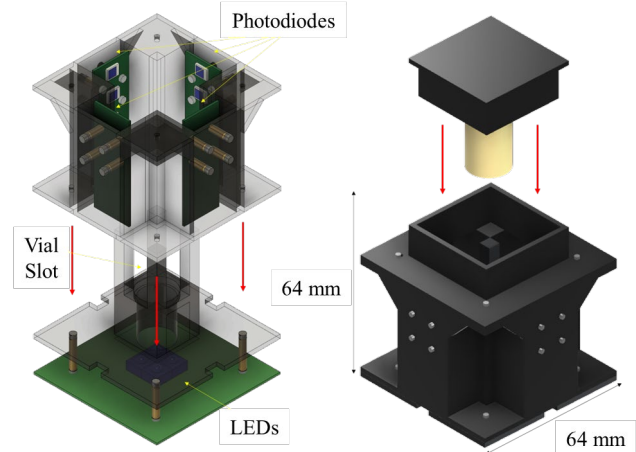


Fig. 4. Architecture of the optoelectronics readout system for small vial detectors.

Blue light LEDs expose vials from the bottom and to collect the side scattered fraction of light, 4 photodiode array boards are mechanically fixed to the top part of the system. After being collimated by holders, side-scattered light is detected radially at 0, 90, 180, and 270 deg to minimize the angular dependence of the response of the readout system and, consequently, to also increase the repeatability of the measurements.

A top cap allows to easily place and remove the vial from the reader, making the user able to process numerous detectors in a short time window; this last feature may be handy in photo-neutron contamination studies, where several vial SDDs may be displaced in the proximity of a LINAC or inside the inserts of a dosimetry phantom, and sequentially read before and after exposure.

Summarizing, the goals of the previous design were the following:

- High sensitivity, accuracy, and precision of the scattered light measurements.
- Low angular dependence of the response.
- Compactness.
- High reading rate of detectors for radiation contamination studies.

Since the readout system is also relatively compact ( $64 \text{ mm} \times 64 \text{ mm} \times 64 \text{ mm}$ ), it is suitable to be used as a personal alarm dosimeter (as a passive detector equipped with an active readout).

#### B. Readout System for Vessel Detectors

Fig. 5 illustrates the design and assembly of 3D printed holders employed for the larger vessel containers. These containers, constructed of tempered glass, can withstand pressures of up to 5 MPa and are produced by Büchi Labortechnik AG.

The active detection volume for each module is  $\text{\O}43 \text{ mm} \times 95 \text{ mm}$ . However, when multiple modules operate in tandem, this active volume can be significantly expanded. For bubble detection during our experiments, we used only two

photodiode boards and two LED boards per module. The main objective of this system was not to achieve high counting accuracy or minimal angular response dependence, but rather to deliver a rapid binary response - indicating the presence or absence of prompt fission neutrons, as could be the case during an active interrogation of a cargo container housing SNMs.

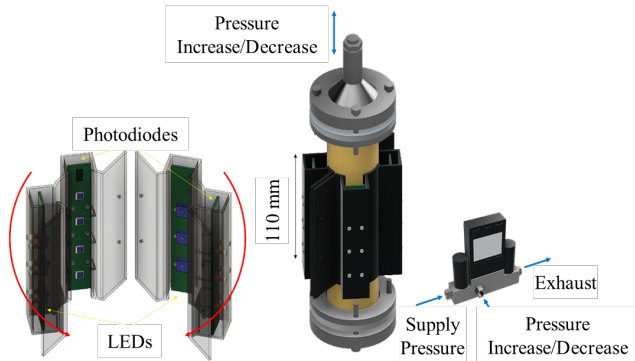


Fig. 5. Architecture of the optoelectronics readout system for large vessel detectors.

Each vessel container is equipped with a digital proportional-integral-derivative (PID) pressure controller from the PCD series by Alicat Scientific. This device serves to adjust the detector's energy threshold response to fast neutrons and, if necessary, repressurize the formed bubbles back into their liquid phase.

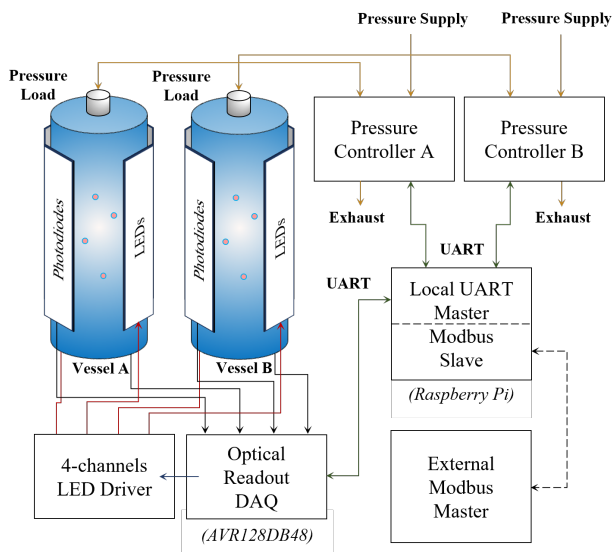


Fig. 6. Architecture of the optoelectronics readout system for large vessel detectors featuring a 100% duty cycle measuring time.

Such a configuration cannot inherently maintain a 100% duty cycle measurement time. As the recompression of bubbles demands several hours, the system is obligated to alternate between a neutron-sensitive low-pressure state and a neutron-insensitive high-pressure state. Furthermore, the base level of scattered light signals depends on both the operative pressure and temperature, as well as the optical properties of the used chemical composition, rendering the system susceptible to long-term drift.

To remedy this and ensure a continuous measurement time, we redesigned the system architecture by utilizing two separate SDDs, each equipped with a dedicated pressure controller (Fig. 6 and Fig. 7). With this setup, one pressure controller maintains a low operative pressure within the first

vessel SDD while the other ensures a high operative pressure within the second vessel, and vice versa.

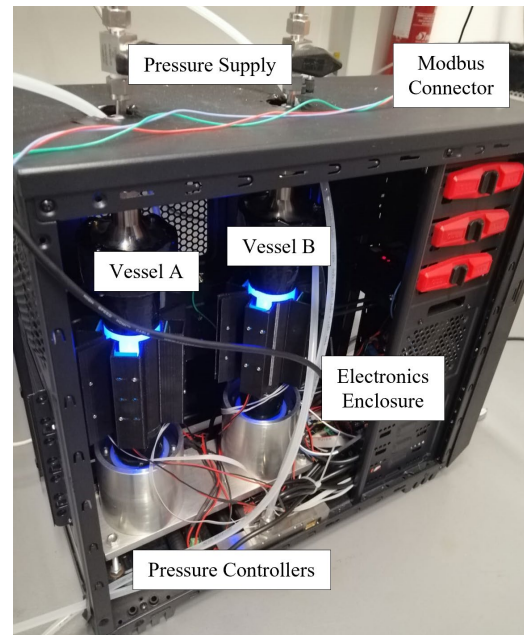


Fig. 7. Realization and assembly of optoelectronics readout system for large vessel detectors featuring a 100% duty cycle measuring time.

The responsibilities of the pressure controllers interchange after a set period, thereby achieving a 100% duty cycle measurement time. Moreover, we incorporated a server for a Modbus RTU communication protocol in the firmware to ensure interface compatibility with external industrial networks. For this task, we employed a commercial single-board computer (Raspberry Pi) and a multi-thread approach for effective control and communication between the devices. The primary threads included a Modbus slave thread for parsing requests from the Modbus master, a data polling thread for querying new data entries from pressure controllers, optoelectronic devices, and a temperature sensor every second, a serial event handler thread for managing received serial data asynchronously and storing them in dedicated data registers, and a main thread for system initialization and operation.

#### IV. RESULTS AND DISCUSSION

In this section, we present the findings from our experiments testing the optoelectronic readout for vial and vessel SDDs. The experiments were conducted at the Laboratory of Nuclear Measurements, Department of Industrial and Civil Engineering, University of Pisa, Italy. Four vial detectors from the same production batch (C318 halocarbon droplets), labeled #1 to #4, were exposed to a  $^{241}\text{Am-Be}$  fast neutron source. This was done to evaluate several key characteristics:

- The signal shape generated by the readout system when bubbles are formed.
- The correlation between the recorded signal and the number of formed bubbles, which can range up to several hundred.
- The SDDs' sensitivity when paired with the optoelectronic readout system.

- The angular sensitivity of the readout system along with the consistency of its measurements.

Fig. 8 illustrates the arrangement used for these measurements.

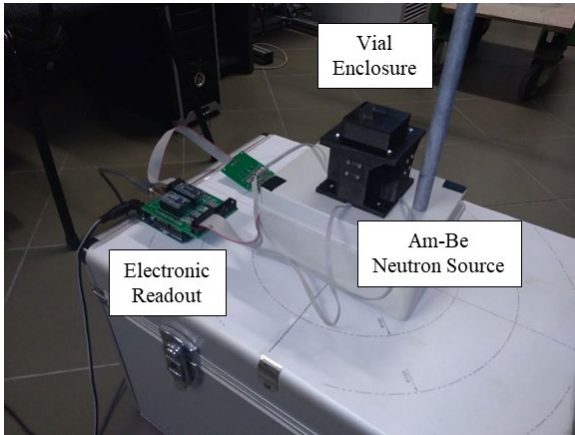


Fig. 8. Setup of the measurements performed to test the response of the readout system for vial SDDs.

Starting from vial #1, once housed within the reader, it was exposed to a  $^{241}\text{Am-Be}$  fast neutron source (67'000 n/s) situated at a 50 mm inter-axis distance for a duration of 4 hours. Before and following each exposure, the light scattering signal was systematically measured. After the signal was successfully recorded, the vial was removed and repositioned 10 times, allowing us to account for any geometric variation that might have been introduced during the repositioning process. This process was executed with a duration of 10 seconds for each respective position. To evaluate the repeatability of our system behavior, the experiment was performed 4 times over, each time re-pressurizing the system to transition the formed bubbles back to the liquid phase. This iterative procedure allowed for a rigorous assessment of the system's consistent performance under identical conditions. All tests were performed in a controlled environment with a consistent temperature of  $23.5 \pm 0.5$  °C.

The reconstructed scattered light signals for the four tests are shown in Fig. 9.

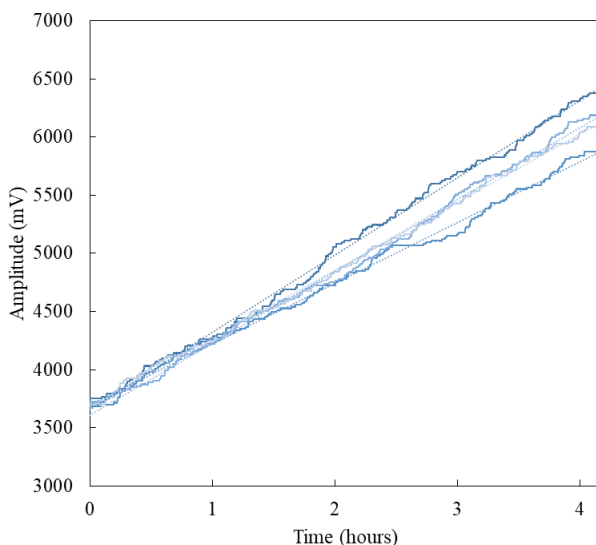


Fig. 9. Response of vial SDD N° 1 during 4-hour exposures to a  $^{241}\text{Am-Be}$  neutron source.

During the 4-hour exposure periods, the combined signals from the photodiode arrays saw an increase of over 2000 mV. Overall, the signal amplitudes demonstrated a notably linear progression over time, and, presuming a consistent vaporization rate, over the number of formed bubbles.

Interestingly, data revealed a significant variance in the increase of signals post-exposure each time, fluctuating roughly between 2100 mV and 2700 mV. This variance corresponded with a significantly different bubble count on each occasion, ranging from 148 to 178 bubbles on average (Table II). These bubble counts were manually determined through offline processing of images captured after the experiment (average value of three pictures taken at 120 deg from each other), using ImageJ image analysis software and its multi-point tool.

TABLE III  
RESPONSE OF VIAL #1 DURING 4-HOURS EXPOSURES TO A  $^{241}\text{Am-Be}$  NEUTRON SOURCE.

Test No	R <sup>2</sup>	$\Delta V$ (mV)	$\Delta N$ (bubbles)	Sensitivity (mV/bubble)
1	> 0.99	$2650.9 \pm 41.7$	$178 \pm 7$	$14.89 \pm 0.63$
2	> 0.99	$2203.5 \pm 93.0$	$148 \pm 5$	$14.88 \pm 0.81$
3	> 0.99	$2452.0 \pm 37.4$	$168 \pm 6$	$14.59 \pm 0.71$
4	> 0.99	$2371.9 \pm 87.5$	$162 \pm 4$	$14.64 \pm 0.65$

According to an ANOVA statistical test, it was found that the sensitivity (mV/bubble) values across the four tests did not significantly differ from each other ( $p > 0.05$ ). As a result, it seemed reasonable to assume a single average sensitivity value for vial #1. The results indicate that the variance in signals observed across the four repetitions can be primarily attributed to differences in the number of bubbles formed post-exposure, rather than inaccuracies in the optoelectronic readout system's readings.

To assess the number of bubbles formed based on the increase of voltage due to the increase of scattered light, the system's response was modeled with an error in variables linear regression model and fitted using the method from York et al. [19] (1):

$$\begin{aligned} \Delta N &= \Delta N^* + \varepsilon_N = k \times \Delta V^* + \varepsilon_N \\ \Delta V &= \Delta V^* + \eta_V \end{aligned} \quad (1)$$

where  $\Delta N$  and  $\Delta V$  are the measured values of bubbles and voltage respectively,  $\Delta N^*$  and  $\Delta V^*$  are the true values of bubbles and voltage respectively,  $\varepsilon_N$  and  $\eta_V$  are the measurement errors, and  $k$  is a calibration factor.

An identical sequence of measurements and analytical procedures were subsequently conducted on vials #2, #3, and #4 (identical chemical composition of C318, comparable droplet sizes, and gel composition). The sensitivity determined by fitting the data for each vial revealed no significant discrepancy among the repeated tests, with ANOVA testing always returning a  $p > 0.05$ . This supports the assumption that it is reasonable to apply a single calibration factor for each vial.

However, a noticeable difference was detected in the average total number of bubbles formed between the different vials, suggesting that the fast neutron detection efficiency might considerably vary between different vials of the same

batch since a Poisson statistic cannot entirely account for this variability.

Furthermore, a significant difference in sensitivity was also discerned ( $p < 0.05$ ), which points towards a potential variation in the optical properties across different detectors (Table III).

TABLE III  
 UNITS FOR SOME MAGNETIC PROPERTIES

Vial ID	Vial Sensitivity (mV/bubble)	$k$ (bubbles/mV)	$N_0$ (bubbles)
#1	14.89 ± 0.37	0.0678 ± 0.0017	0.0 ± 1.3
#2	13.71 ± 0.44	0.0729 ± 0.0024	0.0 ± 1.5
#3	14.17 ± 0.44	0.0702 ± 0.0022	0.0 ± 1.5
#4	15.49 ± 0.46	0.0646 ± 0.0019	0.0 ± 1.8

$N_0$  expresses the number and associated error of estimated bubbles without a voltage increase.

Consequently, it would be advantageous to compute a different calibration factor for each vial, when feasible, to minimize the maximum error when estimating the number of formed bubbles using a post-exposure readout value. Both the accuracy and precision of the measurement are crucial when deducing the number of bubbles from the post-exposure voltage increase. This aspect is particularly pertinent in photo-neutron contamination studies, where a single optoelectronic device could be employed to sequentially read a substantial number of detectors positioned around the area of interest (for instance, inside a dosimetry phantom or near a LINAC).

The system's response's angular dependence was also evaluated. At the end of each exposure, the vials were manually rotated around their longitudinal axis from 0 to 360 degrees in 45-degree increments. The signal was recorded for 10 seconds and subsequently averaged over time. Although the difference between readings taken at various angles is statistically significant when compared to the baseline noise level, the variation is minimal (approximately 2%). This angular dependence of the response needs to be considered, but it's comparable to the error incurred when merely removing and re-positioning the vials. As a result, this aspect doesn't degrade the accuracy or precision of the readout system characterization as described earlier.

## V. CONCLUSIONS

This study demonstrated the potential of optically stimulated SDDs as effective neutron detectors, given their versatile attributes including passive operation, flexible size, and gamma insensitivity. These characteristics, coupled with the capability of tailoring their response to different neutron energies by modifying chemical compositions and operative thermodynamic parameters, position SDDs as promising tools for multiple applications such as homeland security, neutron spectrometry, personnel dosimetry, and radiation safety.

The core of our investigation centered on an optoelectronic readout system for SDDs based on light scattering principles. This system relied on LED light beams interacting with the SDD emulsion, causing measurable attenuation and scattering, subsequently detected by photodiodes. The quantity of scattered light served as a marker for the dose delivered to the detectors.

Our project utilized SDDs in various glass containers and tailored optoelectronic readout systems to meet different

design goals. For vial SDDs, we aimed for high sensitivity, accuracy, precision, linearity, and compactness. These attributes make them ideal for use as an active pocket personal dosimeter and a portable SDDs reader in photo-neutron contamination studies. Conversely, the vessel SDDs system focused on detecting bubble formation within seconds in large volumes and utilized digital pressure controllers to manipulate the operative pressure.

The vial SDDs readout system showed a very linear increase in the amount of scattered light (and hence bubble formation) over time, with minimal differences in sensitivity in repeated tests. Nevertheless, a noticeable difference was observed in the optical readout sensitivity and neutron detection efficiency among the tested vials. These findings highlight the importance of individual calibration for each vial but also suggest the potential for a global calibration factor with a higher readout uncertainty.

The developed system may emerge as a cost-effective candidate for neutron spectrometry after processing the acquired data with deconvolution algorithms.

Overall, our study underscores the potential of SDDs and optoelectronic readouts in various domains and sets the stage for further refinements and applications of this technology.

## REFERENCES

- [1] R. T. Kouzes, J. H. Ely, L. E. Erikson, W. J. Kernan, A. T. Lintereur, E. R. Siciliano, D. L. Stephens, D. C. Stromswold, R. M. Van Ginhoven, and M. L. Woodring, "Neutron detection alternatives to 3He for national security applications," *Nuclear Instruments and Methods in Physics Research Section A: Accelerators, Spectrometers, Detectors and Associated Equipment*, vol. 623, no. 3, pp. 1035-1045, 2010. [Online]. Available: <https://doi.org/10.1016/j.nima.2010.08.021>.
- [2] C. W. E. van Eijk, "Neutron detection and neutron dosimetry," *Radiation Protection Dosimetry*, vol. 110, no. 1-4, pp. 5-13, Aug. 2004. [Online]. Available: <https://doi.org/10.1093/rpd/nch155>.
- [3] R. C. Runkle, A. Bernstein, and P. E. Vanier, "Securing special nuclear material: Recent advances in neutron detection and their role in nonproliferation," *Journal of Applied Physics*, vol. 108, no. 11, p. 111101, Dec. 2010. [Online]. Available: <https://doi.org/10.1063/1.3503495>.
- [4] T. Gozani, "The role of neutron-based inspection techniques in the post 9/11/01 era," *Nuclear Instruments and Methods in Physics Research Section B: Beam Interactions with Materials and Atoms*, vol. 213, pp. 460-463, 2004. [Online]. Available: [https://doi.org/10.1016/S0168-583X\(03\)01590-8](https://doi.org/10.1016/S0168-583X(03)01590-8).
- [5] T. Roy, Y. Kashyap, M. Shukla, P. Singh, and R. Baribaddala, "Fast neutron interrogation of special nuclear material using differential die-away technique," *Applied Radiation and Isotopes*, vol. 176, p. 109896, 2021. [Online]. Available: <https://doi.org/10.1016/j.apradiso.2021.109896>.
- [6] R. Sarkar, B. K. Chatterjee, B. Roy, and S. C. Roy, "Radiation detection by using superheated droplets," *Radiation Physics and Chemistry*, vol. 75, no. 12, pp. 2186-2194, 2006. [Online]. Available: <https://doi.org/10.1016/j.radphyschem.2005.10.007>.
- [7] F. d'Errico, "Status of radiation detection with superheated emulsions," *Radiation Protection Dosimetry*, vol. 120, no. 1-4, pp. 475-479, Sep. 2006. [Online]. Available: <https://doi.org/10.1093/rpd/ncj018>.
- [8] F. d'Errico, "Radiation dosimetry and spectrometry with superheated emulsions," *Nuclear Instruments and Methods in Physics Research Section B: Beam Interactions with Materials and Atoms*, vol. 184, no. 1-2, pp. 229-254, 2001. [Online]. Available: [https://doi.org/10.1016/S0168-583X\(01\)00730-3](https://doi.org/10.1016/S0168-583X(01)00730-3).
- [9] D. T. Bartlett, R. Tanner, and D. J. Thomas, "Active neutron personal dosimeters - A review of current status," *Radiation Protection Dosimetry*, vol. 86, no. 2, pp. 107-122, 1999. [Online]. Available: <https://doi.org/10.1093/oxfordjournals.rpd.a032930>.
- [10] F. d'Errico and A. J. Bos, "Passive detectors for neutron personal dosimetry: state of the art," *Radiation Protection Dosimetry*, vol. 110, no. 1-4, pp. 195-200, 2004. [Online]. Available: <https://doi.org/10.1093/rpd/nch129>.
- [11] S. C. Roy, "Superheated liquid and its place in radiation physics," *Radiation Physics and Chemistry*, vol. 61, no. 3-6, pp. 271-281, 2001.

- [Online]. Available: [https://doi.org/10.1016/S0969-806X\(01\)00250-X](https://doi.org/10.1016/S0969-806X(01)00250-X).
- [12] R. E. Apfel and Y. C. Lo, "Practical neutron dosimetry with superheated drops," *Health Physics*, vol. 56, no. 1, pp. 79-83, 1989. [Online]. Available: <https://doi.org/10.1097/00004032-198901000-00007>.
- [13] S. Gao, G. Zhang, B. Ni, C. Zhao, H. Zhang, Y. Guan, Z. Chen, C. Xiao, C. Liu, and C. Liu, "Acoustic response of superheated droplet detectors to neutrons," *Nuclear Instruments and Methods in Physics Research Section A: Accelerators, Spectrometers, Detectors and Associated Equipment*, vol. 668, pp. 21-25, 2012. [Online]. Available: <https://doi.org/10.1016/j.nima.2011.11.006>.
- [14] F. d'Errico, R. Nath, S. K. Holland, M. Lamba, S. Patz, and M. J. Rivard, "A position-sensitive neutron spectrometer/dosimeter based on pressurized superheated drop (bubble) detectors," *Nuclear Instruments and Methods in Physics Research Section A: Accelerators, Spectrometers, Detectors and Associated Equipment*, vol. 476, no. 1-2, pp. 113-118, 2002. [Online]. Available: [https://doi.org/10.1016/S0168-9002\(01\)01403-6](https://doi.org/10.1016/S0168-9002(01)01403-6).
- [15] R. E. Apfel, "The superheated drop detector," *Nuclear Instruments and Methods*, vol. 162, no. 1-3, pp. 603-608, 1979. [Online]. Available: [https://doi.org/10.1016/0029-554X\(79\)90735-3](https://doi.org/10.1016/0029-554X(79)90735-3).
- [16] R. E. Apfel, S. C. Roy, and Y.-C. Lo, "Prediction of the minimum neutron energy to nucleate vapor bubbles in superheated liquids," *Physical Review A*, vol. 31, no. 5, pp. 3194-3198, 1985. [Online]. Available: <https://doi.org/10.1103/PhysRevA.31.3194>.
- [17] T. Wriedt, "Mie theory: a review," in *The Mie Theory: Basics and Applications*, 2012, pp. 53-71.
- [18] L. Zhao, et al., "Temperature-Dependent Efficiency Droop in GaN-Based Blue LEDs," *IEEE Electron Device Letters*, vol. 39, no. 4, pp. 528-531, April 2018, doi: 10.1109/LED.2018.2805192.
- [19] D. York, N. M. Evensen, M. López Martínez, and J. De Basabe Delgado, "Unified equations for the slope, intercept, and standard errors of the best straight line," *American Journal of Physics*, vol. 72, no. 3, pp. 367-375, March 2004. [Online]. Available: <https://doi.org/10.1119/1.1632486>.